

**Supplementary Information for**

**Non-invasive imaging of tumor progression, metastasis and fibrosis using a  
nanobody targeting the extracellular matrix**

Noor Jailkhani<sup>a</sup>, Jessica R Ingram<sup>b, 1</sup>, Mohammad Rashidian<sup>c</sup>, Steffen Rickelt<sup>a</sup>, Chenxi Tian<sup>a</sup>, Howard Mak<sup>a</sup>, Zhigang Jiang<sup>a</sup>, Hidde L. Ploegh<sup>c</sup>, and Richard O. Hynes<sup>a, d, 2</sup>

<sup>a</sup>Koch Institute for Integrative Cancer Research, Massachusetts Institute of Technology, Cambridge, MA 02139, USA; <sup>b</sup>Department of Cancer Immunology and Virology, Dana Farber Cancer Institute, Boston, MA 02115, USA; <sup>c</sup>Program in Molecular and Cellular Medicine, Boston Children's Hospital, Boston, MA 02115, USA; <sup>d</sup>Howard Hughes Medical Institute, Chevy Chase, MD 20815, USA

<sup>1</sup>Deceased

<sup>2</sup>Corresponding author. Email: [rohynes@mit.edu](mailto:rohynes@mit.edu)

**This PDF file includes:**

Supplementary text  
Figs. S1 to S7  
Captions for movies S1 to S33  
References for SI reference citations

**Other supplementary materials for this manuscript include the following:**

Movies S1 to S33

## **Supplementary Text**

### **Materials and Methods**

#### **Preparation of ECM immunogen mixture**

To obtain a broad spectrum of antibodies against extracellular matrix (ECM) proteins we immunized one alpaca (A) with a ‘cocktail’ of human and murine ECM peptides and proteins. We selected a set of thirty-one peptides and nine purified proteins that were all ECM-associated and of prior interest from earlier proteomic analyses. For the majority of the fifteen proteins selected (AGRN, COMP, HMCN1, LAYN, LOXL2, LTBP1-3, POSTN, SERPINE2, SNED1, Sned1, SPARC, SPP1, TIMP1, THBS2), two unique peptides (~20-25mers) were chemically synthesized (in collaboration with R. Cook, Biopolymers and Proteomics Core facility, Koch Institute, Cambridge, MA). Peptides were coupled to keyhole limpet hemocyanin (KLH, ThermoFisher Scientific) following manufacturers’ recommended protocols and mixed with commercially available purified proteins, i.e., human collagens COLI, COLIII, COLIV (Advanced BioMatrix) and COLV (Sigma), and osteopontin (SPP1, ThermoFisher Scientific). In addition, tenascins C and W (TNC and TNW, kindly provided by Dr. R. Chiquet, Friedrich Miescher Institute for Biomedical Research, Basel, Switzerland) and protein fragments of fibronectin (FN) splice variants FN-EIIIA and FN-EIIIB (previously made in the Hynes laboratory (1, 2) were used. Three separate alpacas (B, C, D) were immunized with ECM-enriched samples prepared from anonymized patient samples of colorectal cancer metastases to the liver (B, courtesy of Dr. Kenneth Tanabe, Massachusetts General Hospital, Boston, USA) or triple-negative breast cancer metastases to the lung and liver (C and D, courtesy Dr. Saraswati Sukumar, Johns Hopkins School of Medicine). The detailed ECM analysis by mass spectrometry and preparation of libraries B, C and D from these latter immunizations will be reported elsewhere.

#### **Alpaca immunization and phage-display library generation**

Alpacas were immunized by Dr. Steven Purdy (UMass, Amherst, MA) using a protocol approved by the UMass, Amherst and MIT’s Institutional Animal Care and Use Committees (IACUC). To generate VHHs specific to disease ECM, alpacas were

immunized with either a cocktail of ECM proteins/domains/peptides (described above) or ECM-enriched preparations derived from patient samples. After four immunizations, the peripheral B-lymphocytes were isolated and a phage-display library was generated using previously described methods (3, 4). Briefly, using the RNeasy Plus Mini Kit (Qiagen), RNA was extracted from  $\sim 10^6$  cells and used for first-strand cDNA synthesis using three different primer sets (oligo[dT]; random hexamers, and primers specific for the constant region of the alpaca heavy chain gene AICH2 and AICH2.2). VHH sequences were amplified by PCR using primers specific for alpaca VHH genes, digested with NotI-HF and Asc-I (NEB), gel-purified, ligated into the M13-based phage display vector (pD vector) and transformed into TG1 *E. coli* cells (Agilent) by electroporation. Ninety-six individual colonies were picked and sequenced for assessment of library diversity. The libraries were pooled and stored as glycerol stocks at  $-80^{\circ}\text{C}$ . FN-EIIIB specific VHHs were selected by panning library A against recombinantly expressed FN-EIIIB domain, using methods described previously (5). To produce phage, the library was inoculated in 100ml SOC medium containing 50  $\mu\text{g/ml}$  ampicillin and allowed to grow at  $37^{\circ}\text{C}$  until mid-log phase. 1 ml of  $10^{13}$  pfu/ml VCMS helper phage was added and 2 hours after incubation at  $37^{\circ}\text{C}$ , cells were harvested and re-suspended in 100 ml 2YT medium supplemented with 0.1% glucose/100  $\mu\text{g/ml}$  Amp/ 70  $\mu\text{g/ml}$  kanamycin and grown overnight at  $30^{\circ}\text{C}$  in a shaker incubator. This allows production of phages that display the VHHs as a pIII fusion protein. The cells were centrifuged for 20 minutes at 8000rpm and phages were precipitated at  $4^{\circ}\text{C}$  by addition of 1% PEG-6000, 500 mM NaCl to the supernatant. The phage pellet was re-suspended in PBS.

### **Selection of anti-EIIIB VHHs by phage display**

VHHs specific for the EIIIB domain of FN were selected following methods previously described (4, 5). Briefly, 100  $\mu\text{g}$  of recombinant FN-EIIIB was biotinylated on primary amines by addition of Chromalink NHS-biotin reagent (Solulink) in 100 mM sodium phosphate, pH 7.4, 150 mM NaCl using the manufacturer's protocol. 100  $\mu\text{l}$  of MyOne Streptavidin T1 Dynabeads (Life Technologies) were washed with PBS, blocked with 2% (wt/vol) BSA (Sigma) in PBS for 1 hour and then incubated (with agitation) with 20  $\mu\text{g}$  of biotinylated protein in 2%BSA/PBS for 30 minutes at  $25^{\circ}\text{C}$ . After washing beads three

times with PBS, 200  $\mu$ l of prepared phage ( $10^{14}$  pfu/ml) in PBS (with 2% wt/vol BSA) were added to the beads and incubated for 1 hour at RT. After 15 washes with 1 ml PBS, 0.1% Tween-20, phage were eluted with 500  $\mu$ l of a saturated culture of ER2738 *E. Coli* (New England BioLabs) for 15 minutes at 37°C and then with 500  $\mu$ l of 0.2 M glycine, pH 2.2 for 10 minutes at 25°C. The glycine elution was neutralized and pooled with eluted *E. coli*; plated on 2YT plates supplemented with 2% (wt/vol) glucose, 5  $\mu$ g/ml tetracycline, and 10  $\mu$ g/ml ampicillin and incubated overnight at 37°C. The resulting library was scraped and pooled and either stored as a glycerol stock or used for a second round of panning in which bait-protein was reduced to 2  $\mu$ g, phage concentration was reduced to 2  $\mu$ l of  $10^{14}$  pfu/ml and incubation time of beads with phage selected in the first round of panning was reduced to 15 minutes. 96 individual colonies were picked and grown in 96-well plates and induced with IPTG overnight. The supernatant containing VHHs was added to EIIIB-coated (5  $\mu$ g/ml) 96-well ELISA plates and bound clones were detected with anti-E-Tag-HRP antibodies (Bethyl Laboratories) and the chromogenic substrate TMB (Sigma).

### **VHH protein expression and purification**

VHH sequences were sub-cloned into pHEN6 periplasmic expression vector with a C-terminal LPETG sortase motif followed by a 6-His tag and expressed in WK6 *E. coli* cells. Protein expression was induced at  $OD_{600} = 0.6$ , for 16 hours at 30°C with 1 mM IPTG followed by osmotic shock to release the periplasmic fraction which was purified using Ni-NTA beads (Qiagen) and size-exclusion chromatography (Superdex 75 16/600 column; GE Healthcare). Peak fractions were tested by SDS/PAGE followed by Coomassie blue staining, pooled and concentrated using Amicon 10-kDa molecular weight cut-off filtration unit (EMD Millipore) and stored at -80°C.

### **Immunofluorescence**

Aortic endothelial cells (AECs) that were either wild-type or knock-out for the EIIIA and EIIIB domains of FN were seeded on coverslips, grown to confluence and allowed to grow for an additional 2-3 days to allow ECM deposition. Cells were washed with PBS, blocked with 2% ovalbumin (1 hour at 37°C) before incubating with the following

primary antibodies; NJB2-Biotin, AM3 (Hynes lab mouse anti-EIIIB monoclonal), anti-FN polyclonal (Abcam) for 2 hours at 37°C. After three washes with PBS, cells were fixed with 4% paraformaldehyde in PBS (5 minutes at RT), washed three times with PBS and incubated with Alexa 488 labeled secondary antibodies (Anti-rabbit IgG Alexa 488 and anti-mouse IgG Alexa 488) or streptavidin Alexa 488 (Invitrogen). Following three washes with PBS, coverslips were incubated with 0.5 µg/ml DAPI (10 minutes at RT). Finally the coverslips were washed with PBS and distilled water and mounted onto microscope slides using mounting medium Fluormount-G (SouthernBiotech). Images were acquired using the Axiovert 200 inverted fluorescence microscope (Zeiss) and processed with imaging software ZEN 2 (blue edition) V3.0 en (Jena, Germany).

### **Affinity determination by Bio-Layer Interferometry (BLI)**

$K_D$  determination was done using Bio-layer interferometry (BLI) using an Octet RED96 instrument (Pall ForteBio). The assay was performed in PBS supplemented with 0.05% Tween-20 and 1% recombinant human albumin (Sigma). Biotinylated NJB2 was immobilized on streptavidin-coated BLI biosensor tips by immersing tips in a 100nM solution. The association was analyzed by submerging sensors in different concentrations of analyte (EIIIB domain or FN 7-15 EIIIB domain). Buffer baselines (NJB2 loaded tips without analyte) were subtracted from the data. Data analysis was done using the ForteBio data analysis software (V8.2) to obtain the association and dissociation rate constants using the 1:1 binding model and a global fit analysis.

### **Immunohistochemistry**

Immunohistochemistry (IHC) was performed as described (6). Briefly, all tissues were fixed in 4% formaldehyde in PBS at RT overnight and paraffin-embedded following standard procedures. Consecutive sections (4-6 µm) were prepared using a Leica RM2255 rotary microtome (Leica Biosystems), dried at 60°C for 1 hour and stored at RT. Prior to immunostaining, individual sections were dewaxed, rehydrated and treated with heat-induced epitope-retrieval by incubation in 10 mM sodium-citrate (pH6.0) or 10mM Tris (pH9.0) buffered solutions containing 0.05% Tween at 120°C for 2 minutes using a decloaking chamber (Biocare Medical). To obtain consistent and reliable stainings on all

tissues investigated, an automated staining system (LabVision Autostainer 360, ThermoFisher Scientific) was used. To destroy endogenous peroxidase and alkaline phosphatase activity in the tissue, the sections were pretreated using BLOXALL endogenous enzyme-blocking solution (Vector Laboratories) for 10 minutes. After a blocking step with normal serum, the sections were incubated with the individual primary antibodies for 1 hour followed by secondary ImmPRESS polymer- detection systems (Vector Laboratories) according to the manufacturer's protocol. For IHC with biotinylated nanobodies, streptavidin horseradish-peroxidase or streptavidin alkaline phosphatase conjugates (BD Biosciences) was used instead of the ImmPRESS polymer-detection system. Subsequently, the Vulcan Fast Red Chromogen Kit 2 (red staining; Biocare Medical) or the DAB Quanto System (brown staining; ThermoFisher Scientific) was applied as substrates. Hematoxylin was used as final counterstain. For hematoxylin and eosin (H&E) staining, the Thermo Scientific Shandon Varistain Gemini ES Automated Slide Stainer (ThermoFisher Scientific) was used following standard protocols. Image documentation was performed using the Leica Aperio AT2 slide scanner system. The multiple organ metastatic cancer tissue array (MT2081) was obtained from US biomax.

In the pancreatic cancer model, the determination of stage of progression (PanIN or PDAC) was done post immuno-PET/CT imaging by histopathological analysis performed by a qualified pathologist blinded to the study

### **Two-photon imaging**

Control and tumor-bearing mice were injected with 20 µg of NJB2 labeled with Texas red or Alexa 647 (ThermoFisher Scientific). The mice were euthanized 2 hours post injection; resected organs were placed on a glass coverslip and imaged by two-photon microscopy with an Olympus FV1000 MPE microscope fitted with a SpectraPhysics MaiTai DeepSee laser. Imaging was performed using 840 nm excitation laser and the following filters: second harmonic generation collagen I (425/30 nm), Zs-Green (525/45 nm), Texas red (607/70 nm) and Alexa 647 (672/30 nm) and using a 25 × 1.05 NA water immersion objective with correction lens. Images were acquired as a series of 5 µm Z-stacks (512x512 pixel frames) to different axial depths within the tissues using the

Fluoview FV10-ASW (version 4.1). At least 3 Z series were acquired for each tissue and saved as oif files. The Z stacks were reconstructed and scale bars were added using FIJI (version 1.0).

### **Confocal imaging**

Confocal microscopy was done with an Olympus FV1200 laser scanning confocal microscope with a 10X, 0.4 NA objective and a Hamamatsu ImagEM high-sensitivity camera. Imaging was done using 473 nm (green), 559 nm (red) and 635 nm (far-red) lasers and the following detectors/filters 465-495 nm (Zs-green), 490-540 nm (Texas-red), and 575-675 nm (Alexa 647). Images were acquired using the Olympus acquisition software Fluoview FV10-ASW (version 4.1).

### **Fibrosis induction**

Albino C57BL/6 mice were administered 0.035U of bleomycin sulfate (Selleck Chemicals, S1214) using intra-tracheal delivery methods described previously (7). Sham treated mice were administered PBS. Mice were euthanized after PET/CT imaging either 7 or 14 days after administration and lungs were resected for histopathological examination and IHC.

### **Cell culture**

LM2-TGL-ZsGreen cells were derived from LM2-TGL cells (a kind gift of Dr. Joan Massague, Memorial Sloan Kettering Cancer Center, New York, NY, USA) by retroviral infection with an MSCV-ZsGreen-2A-puro construct described previously (8). 4T1 cells were purchased from ATCC. B16F10 cells were a kind gift from the Irvine Lab (Koch Institute at MIT). To facilitate tumor cell tracking *in vivo* and microscopy, 4T1 and B16F10 cells were infected with MSCV-luciferase-IRES-ZsGreen (pCT14) modified from MSCV-IRES-Hygro as described previously (8) to make 4T1-Luc-ZsGreen and B16F10-Luc-ZsGreen cells. Retro-viral packaging and infection were done as previously described (9). Cells were maintained in HyClone high-glucose Dulbecco's modified Eagle medium (ThermoFisher Scientific), supplemented with 2 mM glutamine and 10% fetal bovine serum (Invitrogen) at 37°C in a 5% CO<sub>2</sub> incubator.

Aortic endothelial cells (AEC) isolated from the aortic intima of EIIIAB<sup>-/-</sup> (AB null) and EIIIAB<sup>+/+</sup> (AB wild-type) mice were a kind gift from the Murphy Lab (UConn, CT, USA). The EIIIAB<sup>-/-</sup> mice have been described previously (10). AECs were maintained in HyClone high-glucose Dulbecco's modified Eagle medium (ThermoFisher Scientific), supplemented with 2 mM glutamine and 10% fetal bovine serum, 10mg/ml endothelial growth supplement (ECGS, Biomedical Technologies) and 25 mg/ml Heparin (Sigma).

### **Mouse strains and animal models**

All mice were housed at the Koch Institute for Integrative Cancer Research and maintained in accordance with protocols approved by the MIT's IACUC. NSG (NOD/SCID/IL2Rg-null), C57BL/6, Albino C57BL/6 and MMTV-PyMT were purchased from Jackson Laboratory. BALB/c mice were purchased from Taconic. FN-EIIB knockout mice have been previously described (11).

For the pancreatic cancer experiments we used KPC (LSL-Kras<sup>G12D/+</sup>; LSL-p53<sup>R172H/+</sup>; Pdx-1-Cre or LSL-Kras<sup>G12D/+</sup>; p53<sup>flox/flox</sup>; Pdx-1-Cre) mice (12, 13). Age-matched littermates with normal pancreas (confirmed by histology) were used as controls. To capture different stages of PDAC progression we imaged mice between the ages of 2-8 months.

Alpacas (*V. pacos*) were maintained at a local farm and immunized and bled by following a protocol authorized by the University of Massachusetts (Amherst) Veterinary School's IACUC and the MIT IACUC.

### ***In vivo* tumor formation and metastasis**

For xenograft experiments the following strains of mice were used; NSG mice for human triple-negative breast cancer cell line LM2-TGL-ZsGreen, syngeneic BALB/c mice for the murine mammary carcinoma 4T1-Luc-ZsGreen cell line and syngeneic C57BL/6 mice for the murine melanoma B16F10-Luc-ZsGreen cells. For mammary tumor induction, cells were injected in the fourth right mammary fat pad of 8 to 12-week-old female mice. For subcutaneous tumors, B16F10 cells were injected in the right flank of 8 to 12 week old female mice. For pulmonary metastasis experiments, cells were injected



via the lateral tail vein. Tumor and metastases progression was monitored by IVIS imaging.

### **PET/CT data analysis**

Two- and three-dimensional image visualizations of co-registered PET/CT data and quantitative data analysis were done using the VivoQuant software, version 3.5 (Invivo). All PET/CT images are represented as maximum intensity projections of all slices. 3-D regions of interest (ROIs) were drawn around the indicated organs and PET standardized uptake values (SUV) were calculated as  $SUV = \text{Concentration in ROI} / (\text{Injected dose} / \text{Mouse body weight})$ . For mice with lung metastases and fibrosis, ROIs were drawn around whole lungs using CT for reference. For the fibrosis model, ROIs were also drawn around regions with clear  $^{64}\text{Cu-NJB2}$  signal (i.e. “fibrosis”). Images were scaled to PET-SUV unless otherwise indicated. Quantification of radioactivity was decay corrected.

### **Statistical analysis**

Statistical analysis was done using “n” values and tests indicated in the figures or legends. Graphpad prism (version 6.0) was used for statistical analysis and the following P values were considered:  $P > 0.05$  (not significant),  $P \leq 0.05$  (\*),  $P \leq 0.01$  (\*\*),  $P \leq 0.001$  (\*\*\*) and  $P \leq 0.0001$  (\*\*\*\*).

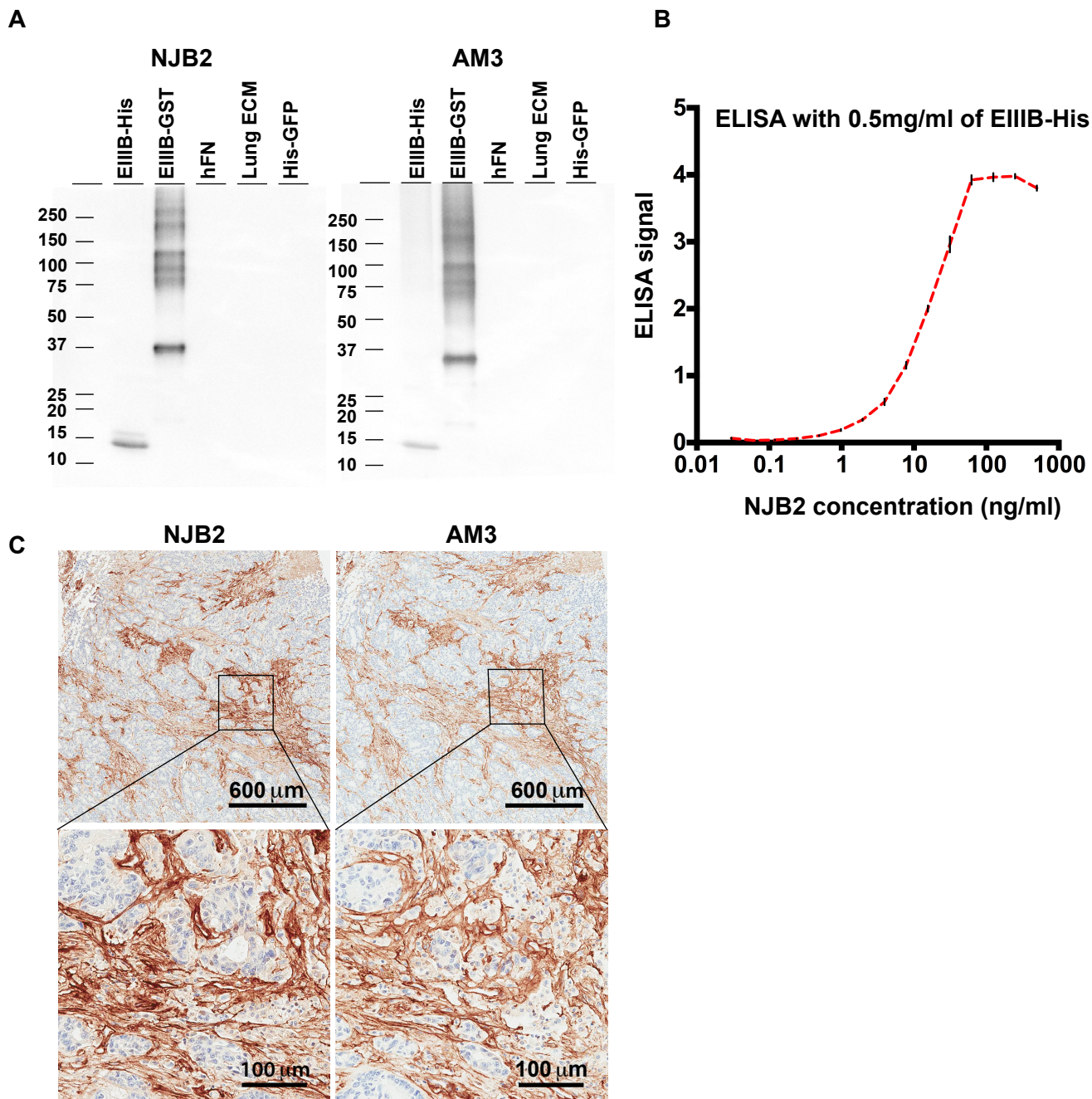


**Fig S1. *In vitro* validation of NJB2.** (A) NJB2-biotin bound specifically to all fragments containing EIIIB but did not bind negative controls, human serum fibronectin (hFN), normal murine lung ECM extract or His-GFP in immunoblot. These results corroborate those observed with the AM3 antibody ( $\alpha$ -EIIIB mouse monoclonal). NJB2-biotin also recognized EIIIB-His in ELISA (B) and FN-containing EIIIB in immunohistochemistry on tissue sections of human colorectal cancer metastases to the liver (C).

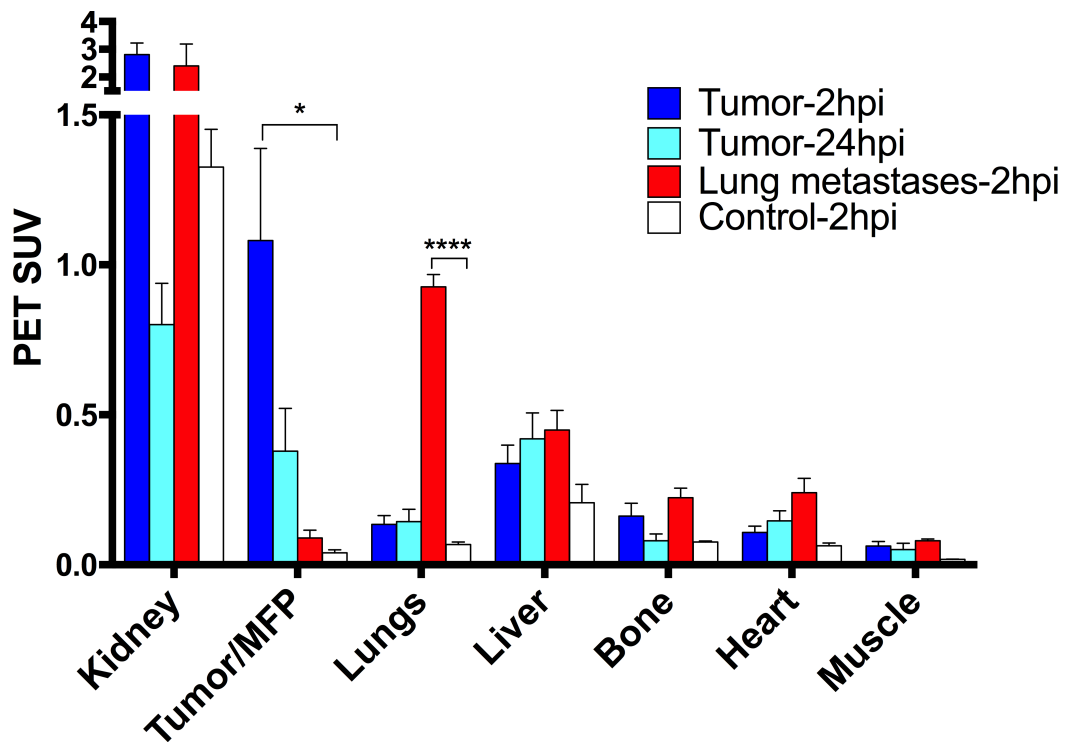


**Fig S2. Quantification of *in vivo* PET-SUV in a breast cancer model.** Decay corrected radioactivity *in-vivo* calculated as PET SUV at 2 and 24 hours after injection of  $^{64}\text{Cu}$ -NJB2 for the indicated organs (blue bars: mice bearing primary tumors; red bars: mice with lung metastases and white bars: controls). Data were analyzed using one-way ANOVA, followed by post-hoc Tukey's multiple comparison tests. n=3 for mice with primary tumors, n=4 for mice with lung metastases and n=2 for control NSG mice. hpi, hours post injection. MFP, mammary fat pad.

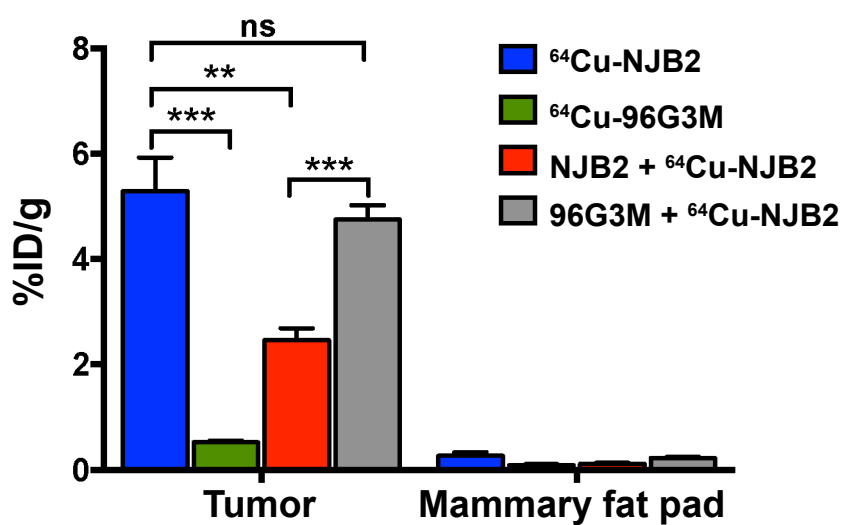
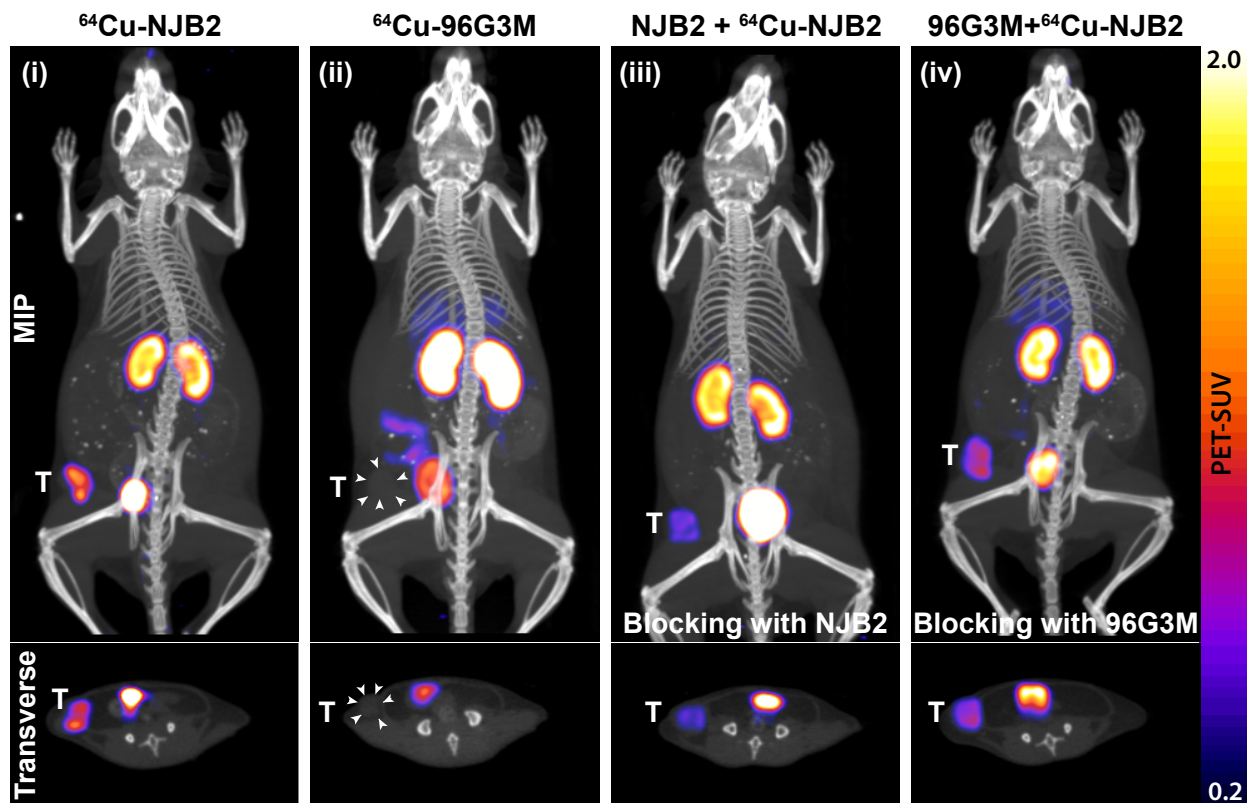


**Fig S3. Specificity testing for the NJB2 nanobody.** Representative PET-CT images of mice with orthotopic tumors derived from LM2 TNBC cells injected with (i)  $^{64}\text{Cu-NJB2}$  (ii)  $^{64}\text{Cu-96G3M}$  (iii) NJB2 (unlabeled) prior to imaging with  $^{64}\text{Cu-NJB2}$  or (iv) 96G3M (unlabeled) prior to imaging with  $^{64}\text{Cu-NJB2}$ . Tumors were resected for ex-vivo radioactivity counts and the contralateral mammary fat pads were used as controls. (Below) *Ex-vivo* biodistribution of PET tracer in resected tumors and contralateral mammary fat pads of indicated mice (150 minutes after injection) expressed as percent of injected dose per gram of tissue (%ID/g) (mean  $\pm$  SE). Data were analyzed by two-tailed unpaired T-test.  $n=4$  for each group. MIP, maximum intensity projection. T, tumor.

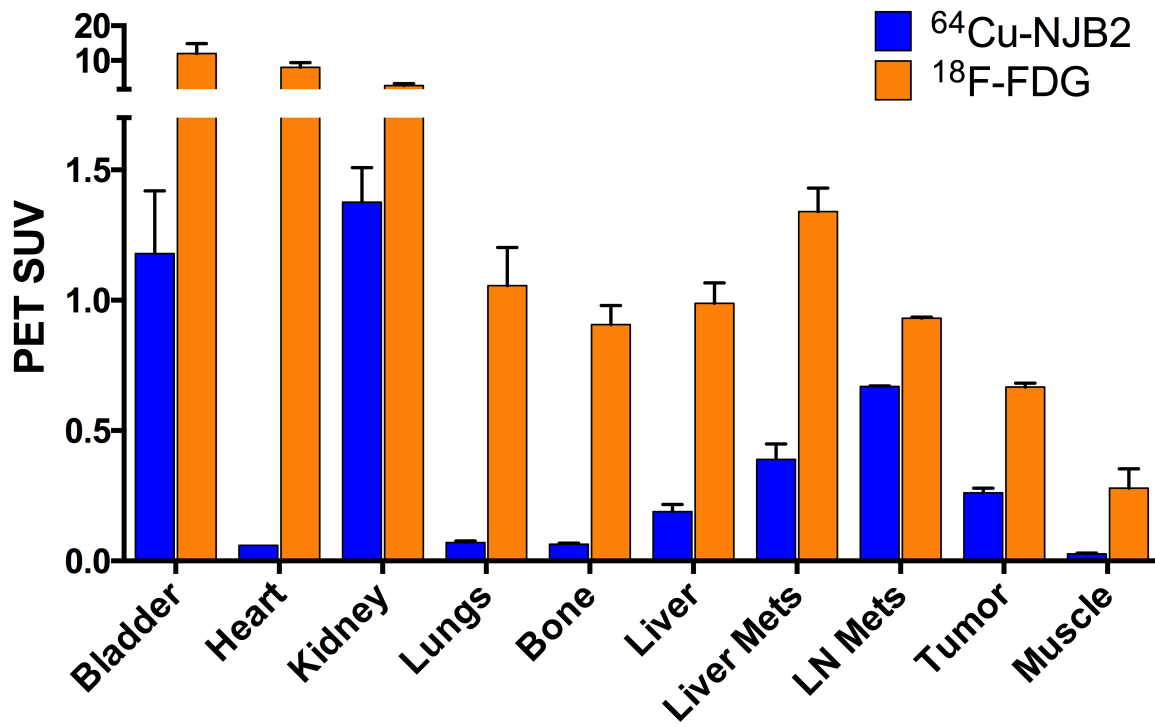
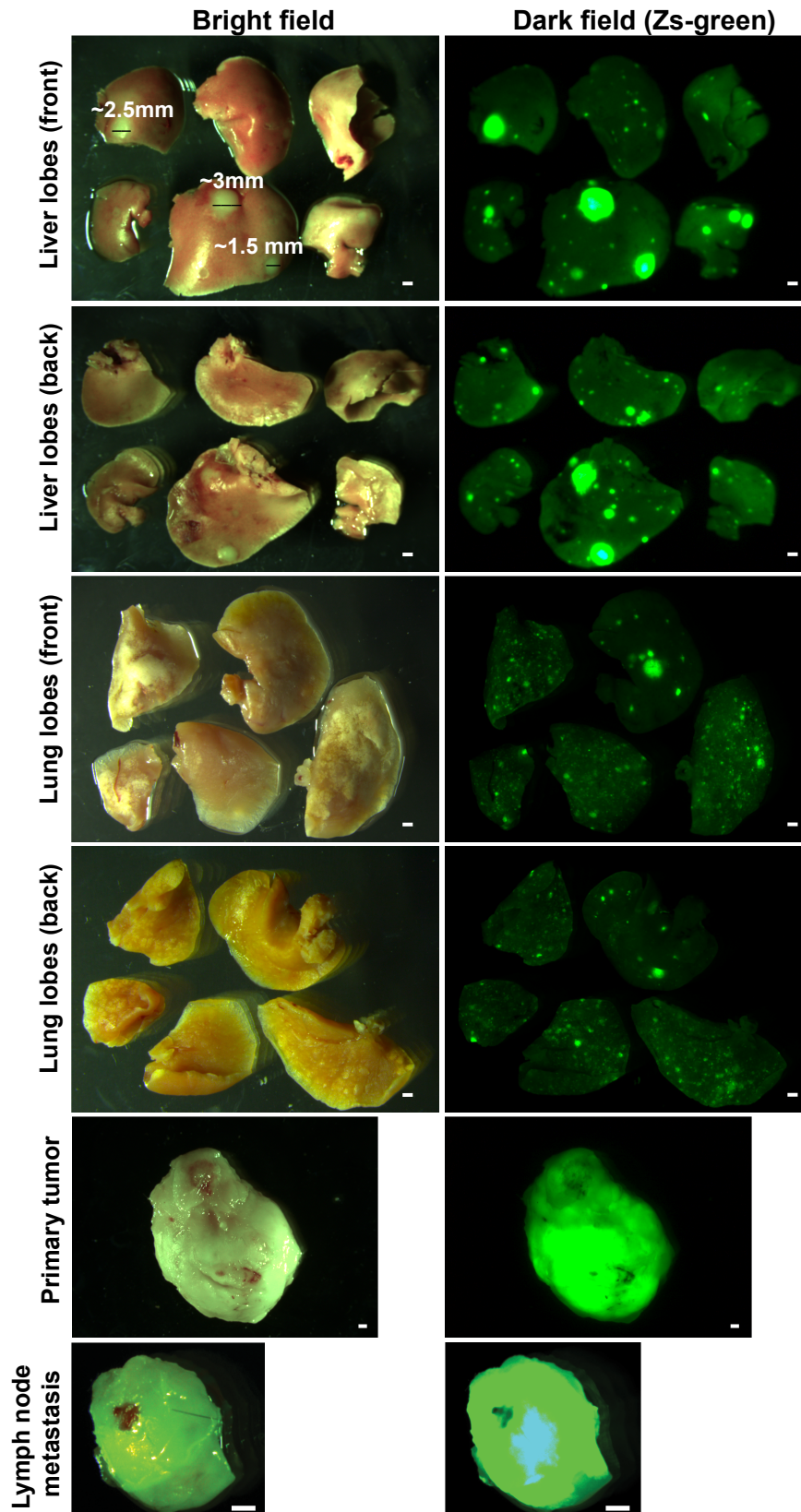
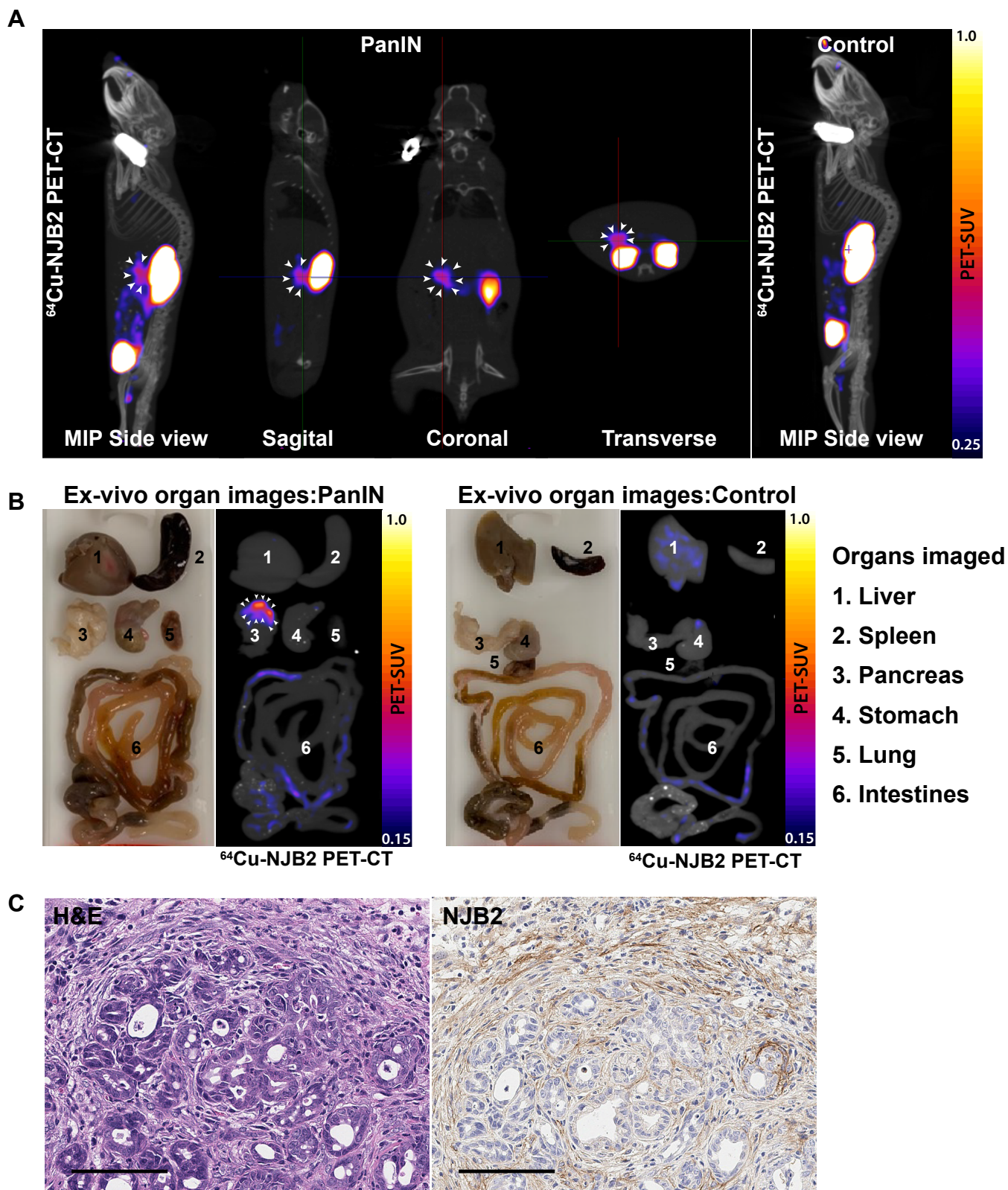


Fig S4. Quantification of *in vivo* PET SUV for  $^{64}\text{Cu-NJB2}$  and  $^{18}\text{F-FDG}$ .



**Fig S5. Fluorescence imaging of organs with metastases.** Bright field and fluorescence microscopy images of primary tumor and organs with distant metastases from a mouse with an orthotopic tumor derived from LM2-TGL-ZsGreen cells imaged in Fig. 3A. Metastases were not observed in other organs. Scale bars, 1mm.



**Fig S6. Ex-vivo imaging of organs from PanIN bearing mice.** (A) Representative PET-CT images of a control mouse and a mouse with PanINs imaged with  $^{64}\text{Cu-NJB2}$ . The signal from the pancreas with PanINs is indicated with arrows. (B) Representative white field and corresponding PET-CT images of organs excised from PanIN bearing and control mice imaged in (A). Clear PET signals are visible from the pancreas of the mouse with PanINs.  $n=4$  for each group. (C) H&E staining and immunohistochemistry with NJB2-biotin of pancreas from mice imaged in (A) confirm PanIN staging and EIIIB expression. Scale bars, 100  $\mu\text{M}$ .

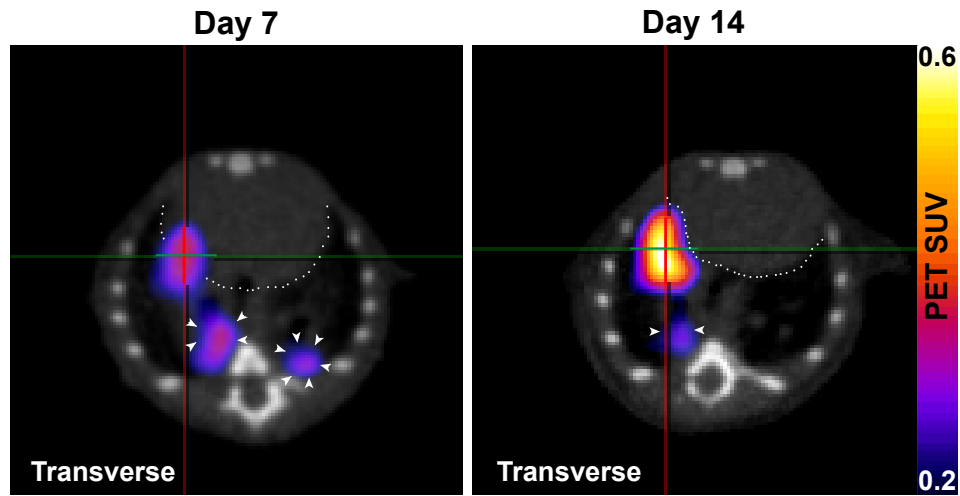


**Fig S7A. Transverse slices of PET/CT images from figure 5.** The cross-hairs indicate the location of a fibrotic lesion within the lung lobes next to the heart. Additional lesions are marked by arrows. The heart is highlighted with dotted lines.

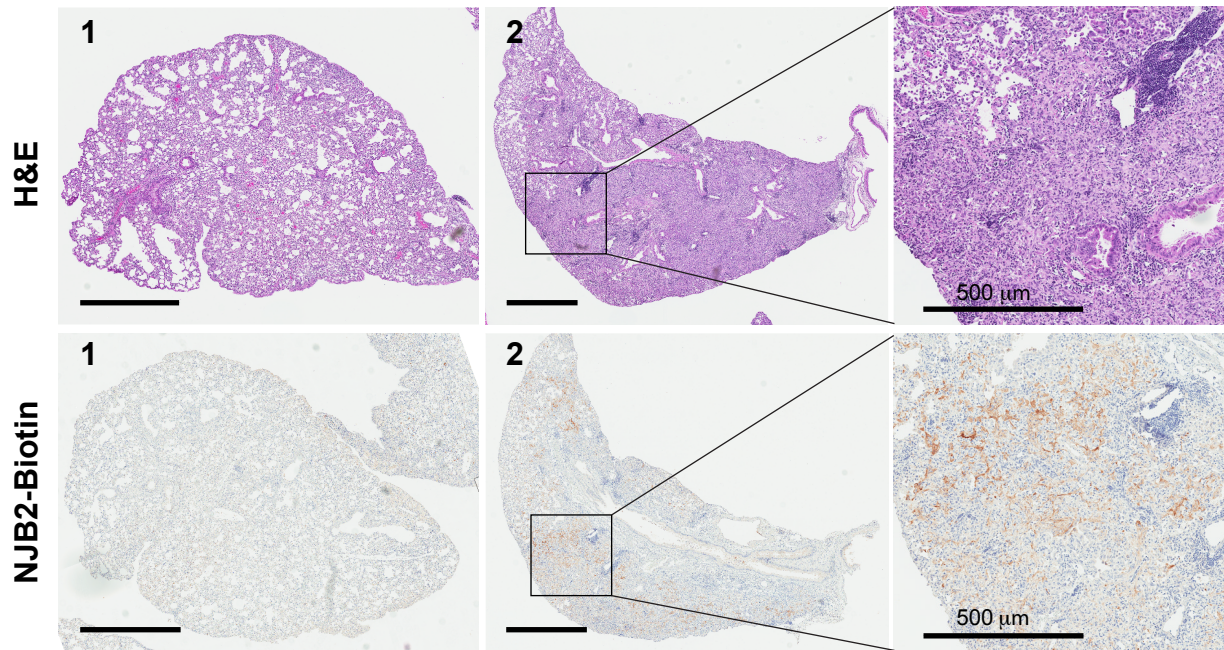


**Fig S7B. Expression of FN-EIIIB is heterogeneous in lung fibrosis.** H&E staining and immunohistochemistry with NJB2-biotin in two distinct lung lobes (1 and 2) excised from a mouse 14 days after bleomycin treatment. The extent of fibrosis in different lobes (1 and 2) and EIIIB expression across each lobe is heterogeneous. Scale bars, 1mm (unless otherwise indicated).



## **Supplementary Movies**

**Movie S1.** Representative  $^{64}\text{Cu}$ -NJB2 PET/CT movie of a NSG control mouse

**Movie S2.** Representative  $^{64}\text{Cu}$ -NJB2 PET/CT movie of a NSG mouse with LM2-derived tumors

**Movie S3.** Representative  $^{64}\text{Cu}$ -NJB2 PET/CT movie of a NSG mouse with LM2-derived lung metastases

**Movie S4.** Representative  $^{64}\text{Cu}$ -NJB2 PET/CT movie of a control mouse in an experiment to test NJB2 in a mouse model of spontaneous metastases

**Movie S5.** Representative  $^{64}\text{Cu}$ -NJB2 PET/CT movie of a mouse with distant metastases

**Movie S6.** Representative  $^{18}\text{F}$ -FDG PET/CT of a control mouse in an experiment to test NJB2 in a mouse model of spontaneous metastases

**Movie S7.** Representative  $^{18}\text{F}$ -FDG PET/CT in a mouse model of spontaneous metastases

**Movie S8.** Representative  $^{64}\text{Cu}$ -NJB2 PET/CT movie of a control mouse with normal pancreas

**Movie S9.** Representative  $^{64}\text{Cu}$ -NJB2 PET/CT movie of a mouse with PanIN

**Movie S10.** Representative  $^{64}\text{Cu}$ -NJB2 PET/CT movie of a mouse with PDAC

**Movie S11.** Representative  $^{18}\text{F}$ -FDG PET/CT movie of a control mouse with normal pancreas

**Movie S12.** Representative  $^{18}\text{F}$ -FDG PET/CT movie of a mouse with PanIN

**Movie S13.** Representative  $^{18}\text{F}$ -FDG PET/CT movie of a mouse with PDAC

**Movie S14.** Representative  $^{64}\text{Cu}$ -NJB2 PET/CT movie of MIP of a control C57BL/6 mouse

**Movie S15.** Representative  $^{64}\text{Cu}$ -NJB2 PET/CT movie of MIP of a mouse treated with bleomycin, 7 days post treatment

**Movie S16.** Representative  $^{64}\text{Cu}$ -NJB2 PET/CT movie of all sagittal slices of a mouse treated with bleomycin, 7 days post treatment

**Movie S17.** Representative  $^{64}\text{Cu}$ -NJB2 PET/CT movie of all coronal slices of a mouse treated with bleomycin, 7 days post treatment

**Movie S18.** Representative  $^{64}\text{Cu}$ -NJB2 PET/CT movie of all transverse slices of a mouse treated with bleomycin, 7 days post treatment

**Movie S19.** Representative  $^{64}\text{Cu}$ -NJB2 PET/CT movie of MIP of a mouse treated with bleomycin, 14 days post treatment

**Movie S20.** Representative  $^{64}\text{Cu}$ -NJB2 PET/CT movie of all sagittal slices of a mouse treated with bleomycin, 14 days post treatment

**Movie S21.** Representative  $^{64}\text{Cu}$ -NJB2 PET/CT movie of all coronal slices of a mouse treated with bleomycin, 14 days post treatment

**Movie S22.** Representative  $^{64}\text{Cu}$ -NJB2 PET/CT movie of all transverse slices of a mouse treated with bleomycin, 14 days post treatment

**Movies S23-27.** Representative  $^{64}\text{Cu}$ -NJB2 PET/CT movies of an MMTV-PyMT mouse imaged at ages of 6,8,10,12 and 13 weeks

**Movie S28.** Representative movie of control BALB/c mouse imaged with  $^{64}\text{Cu}$ -NJB2 PET/CT

**Movies S29-30.** Representative  $^{64}\text{Cu}$ -NJB2 PET/CT movies of BALB/c mice with 4T1 derived tumor (S29) and lung metastases (S30)

**Movie S31.** Representative movie of C57BL/6 mouse imaged with  $^{64}\text{Cu}$ -NJB2 PET/CT

**Movies S32-33.** Representative  $^{64}\text{Cu}$ -NJB2 PET/CT movies of a mouse with B16F10 derived tumor (S32) and lung metastases (S33)

## References

1. Bloom L, Ingham KC, & Hynes RO (1999) Fibronectin regulates assembly of actin filaments and focal contacts in cultured cells via the heparin-binding site in repeat III13. *Mol Biol Cell* 10(5):1521-1536.
2. Peters JH, Trevithick JE, Johnson P, & Hynes RO (1995) Expression of the alternatively spliced EIIIB segment of fibronectin. *Cell Adhes Commun* 3(1):67-89.
3. Maass DR, Sepulveda J, Pernthaner A, & Shoemaker CB (2007) Alpaca (Lama pacos) as a convenient source of recombinant camelid heavy chain antibodies (VHHs). *J Immunol Methods* 324(1-2):13-25.
4. Sosa BA, *et al.* (2014) How lamina-associated polypeptide 1 (LAP1) activates Torsin. *Elife* 3:e03239.
5. Ingram JR, *et al.* (2015) Allosteric activation of apicomplexan calcium-dependent protein kinases. *Proc Natl Acad Sci U S A* 112(36):E4975-4984.
6. Rickelt S & Hynes RO (2018) Antibodies and methods for immunohistochemistry of extracellular matrix proteins. *Matrix Biol.*
7. DuPage M, Dooley AL, & Jacks T (2009) Conditional mouse lung cancer models using adenoviral or lentiviral delivery of Cre recombinase. *Nat Protoc* 4(7):1064-1072.
8. Lamar JM, *et al.* (2012) The Hippo pathway target, YAP, promotes metastasis through its TEAD-interaction domain. *Proc Natl Acad Sci U S A* 109(37):E2441-2450.
9. Stern P, *et al.* (2008) A system for Cre-regulated RNA interference in vivo. *Proc Natl Acad Sci U S A* 105(37):13895-13900.
10. Astrof S, Crowley D, & Hynes RO (2007) Multiple cardiovascular defects caused by the absence of alternatively spliced segments of fibronectin. *Dev Biol* 311(1):11-24.
11. Fukuda T, *et al.* (2002) Mice lacking the EDB segment of fibronectin develop normally but exhibit reduced cell growth and fibronectin matrix assembly in vitro. *Cancer Res* 62(19):5603-5610.
12. Hingorani SR, *et al.* (2005) Trp53R172H and KrasG12D cooperate to promote chromosomal instability and widely metastatic pancreatic ductal adenocarcinoma in mice. *Cancer Cell* 7(5):469-483.
13. Westphalen CB & Olive KP (2012) Genetically engineered mouse models of pancreatic cancer. *Cancer J* 18(6):502-510.